

DISTRIBUTION OF SPONTANEOUS CURRENTS ALONG THE SOMATO-DENDRITIC AXIS OF RAT HIPPOCAMPAL CA1 PYRAMIDAL NEURONS

R. COSSART,* J. C. HIRSCH,* R. C. CANNON,† C. DINONCOURT,* H. V. WHEAL,† Y. BEN-ARI,* M. ESCLAPEZ* and C. BERNARD*‡

*INSERM U29-INMED, Parc Scientifique de Luminy, BP 13, 13273 Marseille Cedex 09, France

†Neuroscience Research Group, School of Biological Sciences, Southampton University, Southampton SO16 7PX, UK

Abstract—Excitatory and inhibitory pathways have specific patterns of innervation along the somato-dendritic axis of neurons. We have investigated whether this morphological diversity was associated with variations in the frequencies of spontaneous and miniature GABAergic and glutamatergic synaptic currents along the somato-dendritic axis of rat hippocampal CA1 pyramidal neurons. Using *in vitro* whole cell recordings from somata, apical dendrites and basal dendrites (for which we provide the first recordings) of CA1 pyramidal neurons, we report that over 90% of the spontaneous currents were GABAergic, <10% being glutamatergic. The frequency of spontaneous GABAergic currents was comparable in the soma and in the dendrites. In both somata and dendrites, the Na⁺ channel blocker tetrodotoxin abolished more than 80% of the spontaneous glutamatergic currents. In contrast, tetrodotoxin abolished most dendritic (>90%) but not somatic (<40%) spontaneous GABAergic currents. Computer simulations suggest that in our experimental conditions, events below 40 pA are electrotonically filtered to such a degree that they are lost in the recording noise. We conclude that, *in vitro*, inhibition is massively predominant over excitation and quantitatively evenly distributed throughout the cell. However, inhibition appears to be mainly activity-dependent in the dendrites whereas it can occur in the absence of interneuron firing in the soma. These results can be used as a benchmark to compare values obtained in pathological tissue, such as epilepsies, where changes in the balance between excitation and inhibition would dramatically alter cell behaviour. © 2000 IBRO. Published by Elsevier Science Ltd. All rights reserved.

Key words: excitation, inhibition, basal dendrites, apical dendrites, pyramidal cells, hippocampus.

There is considerable morphological evidence for an heterogeneous distribution of glutamatergic² and GABAergic^{9,16,27} afferent pathways along the somato-dendritic axis of hippocampal CA1 pyramidal cells. There are interneurons specifically targeting the basal dendrites, the perisomatic region, the lower/higher part of the apical dendrites, the distal dendrites of CA1 pyramidal cells or any combination of these regions.^{9,16,27} This morphological heterogeneity seems to have physiological correlates. Evoked perisomatic inhibition preferentially controls neuronal output whereas dendritic inhibition is better suited to modify local information processing in synergy with the complex active properties of dendrites.^{20,24,36} Furthermore, the properties of postsynaptic GABA_A receptors seem to be target- and interneuron-specific.¹

The goal of this study was to test whether the spontaneous excitatory and inhibitory drives continuously received by CA1 pyramidal cells is compartmentalized along their somato-dendritic axis. Until now, spontaneous activity has only been measured in somata. This activity may represent mostly perisomatic events since imperfect space clamp and the complex electrotonic properties in large adult neurons

prevent proper access to dendrites when somatic recordings are performed.^{4,7,34,37,38} Because of this intrinsic limitation, we have attempted to characterize the activity generated by dendritic projecting pathways using dendritic recordings and compare it to the activity generated by perisomatic projecting pathways recorded in somata. In an effort to assess the degree of contamination of synaptic events recorded in the dendrites by somatically generated currents (and vice versa), we have used a realistic computer model of our experimental conditions.

The second goal of this study was to determine the ratio between excitatory and inhibitory drives along the somato-dendritic axis of CA1 pyramidal cells. Somatic recordings of CA1 pyramidal cells indicate that the GABAergic drive occurs at a higher frequency (0.1–50 Hz) than the glutamatergic one (0–1 Hz).^{5,6,11,14,15,19,23,25,30–32} However, in these studies, the ratio could not be calculated because glutamatergic and GABAergic activities were not measured in the same cell. In the present study, this ratio was determined for each recorded CA1 pyramidal cell.

Patch-clamp recordings from somata, apical and basal dendrites of CA1 pyramidal cells were performed *in vitro* to measure spontaneous glutamatergic and GABAergic currents. We report that spontaneous glutamatergic and GABAergic currents are quantitatively evenly distributed along the somato-dendritic axis. Most (90%) of the spontaneous drive received by CA1 pyramidal cells is inhibitory. Most of the excitatory glutamatergic activity is composed of action potential-dependent events. In contrast, action potential-independent GABAergic events are largely present in the perisomatic region and appear to occur at a low probability in the apical or basal dendrites. Computer simulations are consistent with the idea that the recorded currents are mostly local.

‡To whom correspondence should be addressed at: Division of Neuroscience, S700, Baylor College of Medicine, 1 Baylor Plaza, Houston, TX 77030, USA. Tel.: +1-713-798-76-66; fax: +1-713-798-39-46.

E-mail address: cbernard@ltp.neusc.bcm.tmc.edu (C. Bernard).

Abbreviations: ACSF, artificial cerebrospinal fluid; CNQX, 6-cyano-7-nitroquinoxaline-2,3-dione; D-APV, D-2-amino-5-phosphonovaleric acid; EPSC, excitatory postsynaptic current; HEPES, N-2-hydroxyethyl-piperazine-N'-2-ethanesulphonic acid; IPSC, inhibitory postsynaptic current; mEPSC, miniature excitatory postsynaptic current; mIPSC, miniature inhibitory postsynaptic current; PBS, Phosphate-buffered saline; sEPSC, spontaneous excitatory postsynaptic current; sIPSC, spontaneous inhibitory postsynaptic current; TTX, tetrodotoxin.

EXPERIMENTAL PROCEDURES

Experimental procedures conformed with INSERM guidelines.

Slice preparation

Adult home bred male Wistar rats (one-and-a-half to six months old, $n = 29$) were intracardially perfused under chloral hydrate (350 mg/kg, i.p.) anaesthesia with artificial cerebrospinal fluid (ACSF) in which NaCl was replaced by an equimolar concentration of sucrose and hippocampal slices (350- μ m-thick) were prepared with a Leica VT 1000E tissue slicer as previously described.¹⁵ ACSF contained (in mM): 126 NaCl, 3.5 KCl, 26 NaHCO₃, 1.2, NaH₂PO₄ 1.3 MgCl₂, 2 CaCl₂, 10 glucose and was continuously aerated with 95% O₂ and 5% CO₂. The temperature in the submerged recording chamber was maintained at 30–32°C. All efforts were made to minimize animal suffering and to reduce the number of animals used.

Electrophysiological recordings and data analysis

Activity in CA1 principal cells critically depends upon their spatial location⁸ since connectivity patterns of excitatory and inhibitory afferents vary considerably along both septo-temporal and transverse axes.^{2,22} We have thus taken great care to perform our recordings at similar locations (CA1_b in the mid part of the hippocampus along the septo-temporal axis) at a depth ranging from 100 to 200 μ m where neurons retain more synaptic inputs than when they are recorded close to the surface of the slice.^{8,29} The blind patch clamp technique was preferred to visual patch for the following reasons. Recordings of apical dendrites performed under visual control with infrared video-microscopy could only be done close to the surface of the slice, where spontaneous activity occurs at a lower frequency than deeper into the slice. With the infrared video-microscopy technique the thin basal dendrites could not be visualized.

The patch pipettes used to record from either soma, apical or basal dendrites had a resistance of 8–12 M Ω . Internal solution of the following composition was used (in mM): 135 Cs-gluconate, 2 MgCl₂, 0.1 CaCl₂, 1 EGTA, 10 HEPES, 0.5% biocytin pH 7.25. The osmolality of the internal solutions was between 265 and 275 mOsm. During each experiment the series resistance and membrane resistance were checked every 20 or 30 s by a 5-mV/200-ms pulse and were found to be constant throughout the experiment and similar at the two holding potentials used to measure glutamatergic and GABAergic events. Series resistance was 8–20 M Ω (average 12 ± 2) for somatic recordings and 15–50 M Ω (average 21 ± 5) for dendritic recordings; data were not corrected for this error. Cells were kept at –60 mV or +10 mV for the analysis of glutamatergic or GABAergic spontaneous postsynaptic currents, respectively.¹⁵ At the end of each experiment, these currents were blocked by 6-cyano-7-nitroquinoxaline-2,3-dione (CNQX; 10 μ M)/ D-2-amino-5-phosphonvaleric acid (D-APV; 50 μ M) and bicuculline (10 μ M), demonstrating that they were glutamatergic and GABAergic respectively; not shown, but see refs 14 and 15. Signals were fed to an Axopatch 200A amplifier (Axon, Foster City, CA, USA). All data were digitized (10 kHz) with a Labmaster interface card to a personal computer and analysed with Acquis1 program (G. Sadoc, 1994, Biologic, France). Spontaneous synaptic currents were detected by the software on the basis of amplitude and rise time. Typically, the threshold was set at 2.5 pA/ms for IPSCs and 1.0 pA/ms for excitatory postsynaptic currents (EPSCs), two conservative figures allowing the detection of the maximum number of currents. All detected currents were then eye inspected to reject artefactual events. All the experimental values are given as means \pm S.E.M. Parameters were compared with a Student's *t*-test. The ratio values given in the text and in the table correspond to the average of the percent reduction for individual cells.

Morphological procedures

Neurons were filled passively with biocytin for post hoc morphological identification of the recording site.¹⁴ At the end of the electrophysiological recordings, the pipette was slowly removed from the cell whilst applying a gentle positive pressure in order to limit disruption of the neuronal membrane. Slices were fixed overnight at 4°C in a solution containing 4% paraformaldehyde in 0.1 M phosphate buffer (pH 7.4). After fixation, slices were rinsed in PB, cryoprotected in sucrose overnight and quickly frozen on dry ice. Detection of biocytin-filled neurons was performed on unsectioned slices as previously

reported.¹² In brief, slices were pre-treated for 30 min in 1% H₂O₂ in saline phosphate buffer (0.1 M phosphate-buffered saline; PBS, pH 7.4) and incubated for 24 h at 4°C in avidin-biotinylated peroxidase complex (1:100, Vector Laboratories) diluted in PBS containing 0.3% Triton-X-100. After 30-min rinses in PBS, slices were processed with 0.08% 3',3'-diaminobenzidine tetrahydrochloride (DAB, Sigma) and 0.006% H₂O₂ diluted in PBS, rinsed, mounted on gelatine-coated slides and coverslipped in an aqueous medium (Crystal/Mount, Biomed, Foster City, CA, USA). After histological processing, a dent or a hole in the membrane was detected at the approximate location evaluated during the course of an experiment, using the binocular located over the recording chamber.¹⁴ Furthermore, at high magnification, scattered biocytin particles were clearly seen around the hole or the dent. The validation of this technique is described in the result section.

Drugs

CNQX and D-APV were a gift of Novartis (Bern, Switzerland). Biocytin and cadmium were obtained from Sigma and tetrodotoxin (TTX) from Latoxan (Valence, France).

Model simulation voltage-clamp recordings

The simulations used the 3D reconstruction of a CA1 pyramidal cell filled in an adult rat kindly provided by D. Turner (cell # 184 at <http://www.neuro.soton.ac.uk/cells>). The real diameters of dendrites were included. The model had no active conductance but imperfect space clamp was fully taken into account by clamping the cell at the chosen recording site through a series resistance of 8 M Ω . The reversal potential of the membrane leak was set at –40 mV, with its resistance adjusted to 90,000 M Ω /cm² so as to give a steady-state holding current of 250 pA at the soma for a holding potential of +10 mV and an axial resistance and membrane capacitance of 200 Ω /cm and 1 μ F/cm², respectively. The synaptic current was modelled as an ohmic conductance reversing at –60 mV. Its time-course was given by the difference of two exponentials: $G_{\text{syn}} = A(1 - e^{-t/\tau_1})e^{-t/\tau_2}$, where t is in ms. The simulation was repeated for a wide range of amplitudes (a wide range of values for the constant A), of the synaptic conductance and for different sites for the recording electrode and synaptic input. All parameters (including axial resistance and membrane capacitance) were chosen to achieve conservative estimates of the attenuation of currents.

The detection of events was assessed with the same algorithm as was used on the experimental data. Noise was added to the current from the passive simulation and an event was registered if the minimum to maximum change exceeded 12 pA in any 3-ms period during the 5 ms following the event. The noise was generated as an autoregressive process (AR1) of variance 2 pA and regression parameter $a = 0.1$, at discrete time interval of 0.1 ms. That is, for a sequence of gaussian random variables g_i of unit variance, the noise satisfies: $x_{i+1} = ax_i + 2\sqrt{(1-a^2)}g_i$.

These parameters were selected to give a noise spectrum close to that of a representative experiment. In the absence of synaptic events, they give a null detection rate of one event every 1.5 s. For generating detection probability density functions, a hundred random noise trains were used for each event.

RESULTS

Morphological identification of the recording sites

The recording site in the soma or in the dendrites was identified post hoc as a dent or a hole in the membrane. In order to demonstrate that the dent or the hole represents the recording site, the following procedure was used. Dendritic recordings ($n = 3$, Fig. 1A) were performed using infrared imaging as described previously.³⁵ Lucifer Yellow was added to the patch pipette internal solution. The preparation was epi-illuminated through a $\times 40$ water-immersion objective on the stage of an Axioscope Karl Zeiss microscope and Workbench software (Axon Instruments) with a filter of 730 nm. The preparation was excited at 428 nm using Photonics monochromator and the image acquired through a Photonics CCD camera and monitored by Workbench

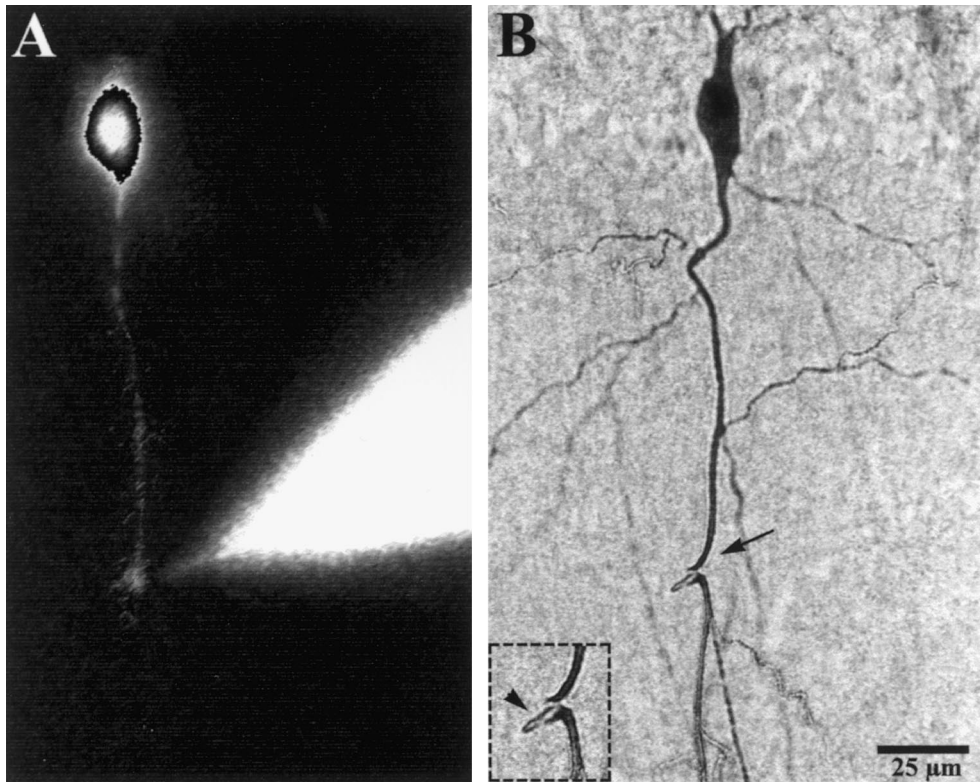


Fig. 1. Post hoc identification of the recording site by a hole or dent left by the pipette. (A) Image of dendrites and soma of a CA1 neuron loaded with Lucifer Yellow via the recording pipette. (B) Same CA1 pyramidal neuron illustrated in A after detection of biocytin. The dent on the apical dendrite (arrow) superimposes with the recording site in A. Note the presence of the broken tip of the pipette (arrowhead) at the level of the dent (inset).

software (Axon Instruments). Subsequent biocytin processing was performed for post hoc morphological identification of the recording site. Biocytin and fluorescent images were then compared. The hole or the dent superimposed with the visualized recording site (Fig. 1B). In the experiment illustrated, the tip of the pipette was broken upon withdrawal, further identifying the exact location of the recording site (Fig. 1B). These results strongly suggest that the dent/hole identified post hoc represents the recording site when blind patch-clamping is performed.

Spontaneous glutamatergic and GABAergic activity in somata and dendrites

Action potential-dependent and -independent glutamatergic and GABA_A receptor-mediated currents were measured at the same recording site at -60 mV and $+10$ mV, respectively. In our experimental conditions, these potentials represent the reversal potentials of GABAergic and glutamatergic currents respectively, in both dendrites and somata. The technique has been detailed elsewhere.^{14,15} The frequencies of the GABAergic

and glutamatergic events recorded in somata, apical and basal dendrites of CA1 pyramidal cells are summarized in Table 1.

Distribution of action potential-dependent and -independent activity in somata

At the reversal potential of GABA_A receptor-mediated events (-60 mV), the frequency of spontaneous excitatory postsynaptic currents (sEPSC) was 0.53 ± 0.16 Hz and was reduced by $89 \pm 9\%$ (Fig. 2B; $n = 8$, $P < 0.001$) after perfusion of the Na⁺ channel blocker TTX ($1 \mu\text{M}$) to isolate action potential-independent currents. Therefore, miniature excitatory postsynaptic currents (mEPSC) are virtually absent in somata. At the reversal potential of glutamatergic events ($+10$ mV), the frequency of spontaneous inhibitory postsynaptic currents (sIPSC) was 16.82 ± 2.21 Hz (Fig. 2C; $n = 10$), i.e. $95 \pm 2\%$ of the combined glutamatergic/GABAergic spontaneous activity. In the presence of TTX the frequency of sIPSCs was decreased to 13.04 ± 4.70 Hz ($P < 0.0001$; Fig. 2C; $n = 8$, Table 1), suggesting that miniature inhibitory postsynaptic current (mIPSC) account for $66 \pm 8\%$ of the GABAergic activity recorded in

Table 1. Distribution of spontaneous excitatory and inhibitory synaptic currents along the somato-dendritic axis of CA1 pyramidal cells

Recording site	AMPA (Hz)	AMPA + TTX (Hz)	GABA (Hz)	GABA + TTX (Hz)	GABA/all
Soma SP ($n = 8$)	0.53 ± 0.16	0.02 ± 0.01 (11%)	16.82 ± 2.21	13.04 ± 4.70 (66%)	95%
Dendrite SR ($n = 9$)	2.01 ± 0.42	0.48 ± 0.10 (24%)	17.29 ± 2.30	1.98 ± 0.58 (12%)	89%
Dendrite SO ($n = 6$)	0.43 ± 0.10	0.04 ± 0.02 (16%)	21.15 ± 3.99	3.65 ± 0.63 (19%)	96%
Soma SO ($n = 5$)	1.96 ± 0.56	0.15 ± 0.07 (10%)	32.09 ± 7.78	11.41 ± 2.06 (27%)	93%

SP stratum pyramidale, SR stratum radiatum, SO stratum oriens. The ratio between the inhibitory drive and the added sum of the excitatory and inhibitory drives is given in the last column.

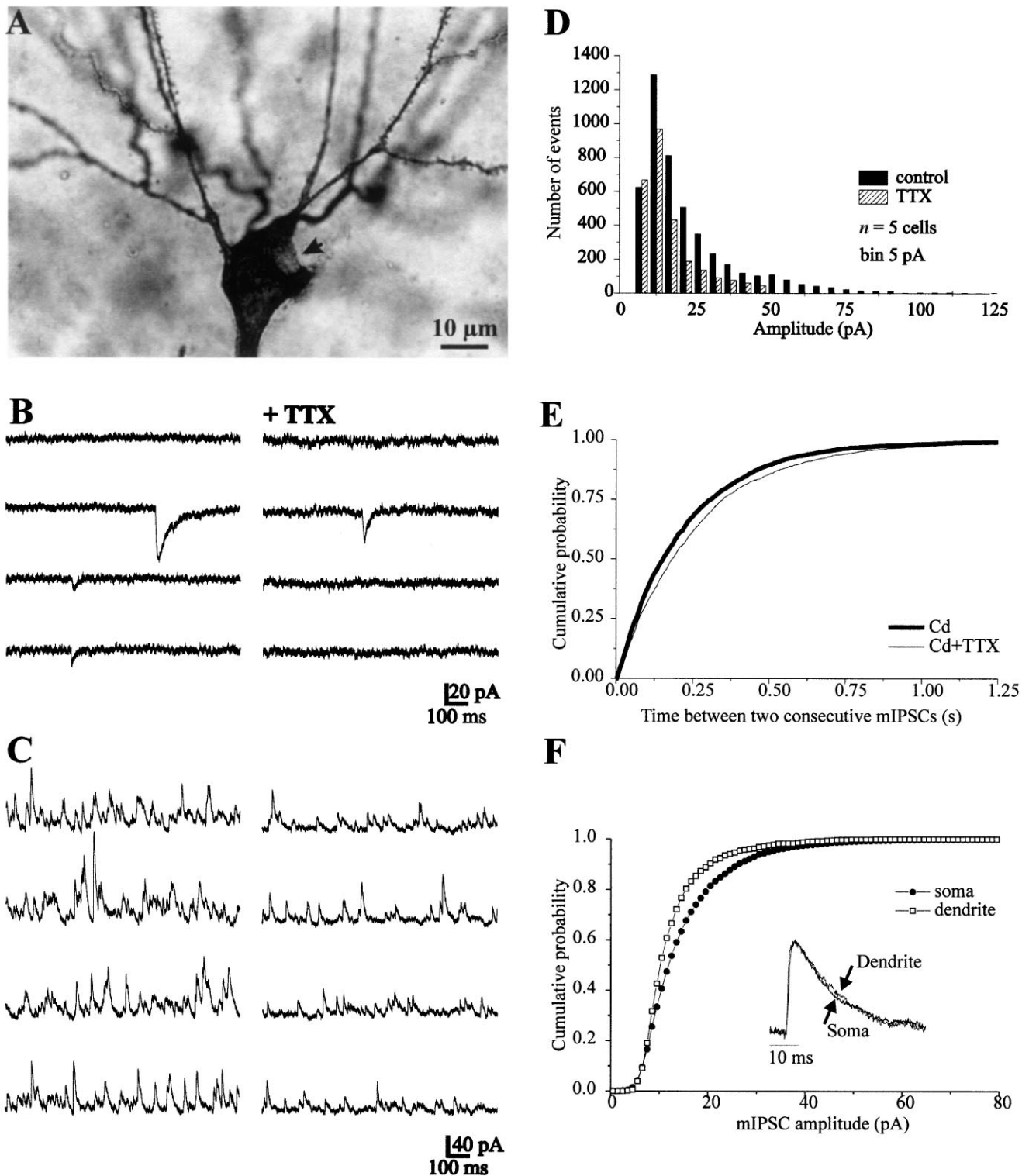


Fig. 2. Distribution of spontaneous and miniature activities in the soma of a CA1 pyramidal neuron. (A) Identification of the recording site (arrow) in the soma of the biocytin-filled neuron. (B, C) The neuron was voltage-clamped at the reversal potential for GABAergic currents (around -60 mV) to record glutamatergic currents and at the reversal potential of glutamatergic currents (around $+10$ mV) to record GABAergic currents. Continuous 4-s recordings of sEPSCs (B) and sIPSCs (C) before (left frames) and after addition of TTX (right frames) are displayed (same type of display used in the next three figures). (B) The frequency of sEPSCs is low in control ACSF and almost nil in TTX, indicating that spontaneous glutamatergic activities in the soma are action potential-dependent. (C) The frequency of sIPSCs is high in control ACSF and remains so in TTX, suggesting that many IPSCs recorded in the soma are due to action potential-independent release of transmitter. In this cell, the ratio of sIPSCs/sEPSCs was 92%. (D) Histogram showing the distribution of amplitudes of IPSCs measured before and after TTX. Note that the proportion of small amplitude IPSCs is similar before and after TTX. (E) Cumulative probability plot of the time interval between two consecutive IPSCs recorded in Cd^{2+} and $\text{Cd}^{2+} + \text{TTX}$. There is a slight left shift suggesting that a few IPSCs measured in Cd^{2+} are TTX-sensitive. (F) Cumulative probability plot of the amplitudes of mIPSCs recorded in somata and dendrites. Note the left shift indicating a decreased frequency of large amplitude events in dendritic recordings. Inset. Normalized mIPSCs measured in somata and dendrites show similar kinetics.

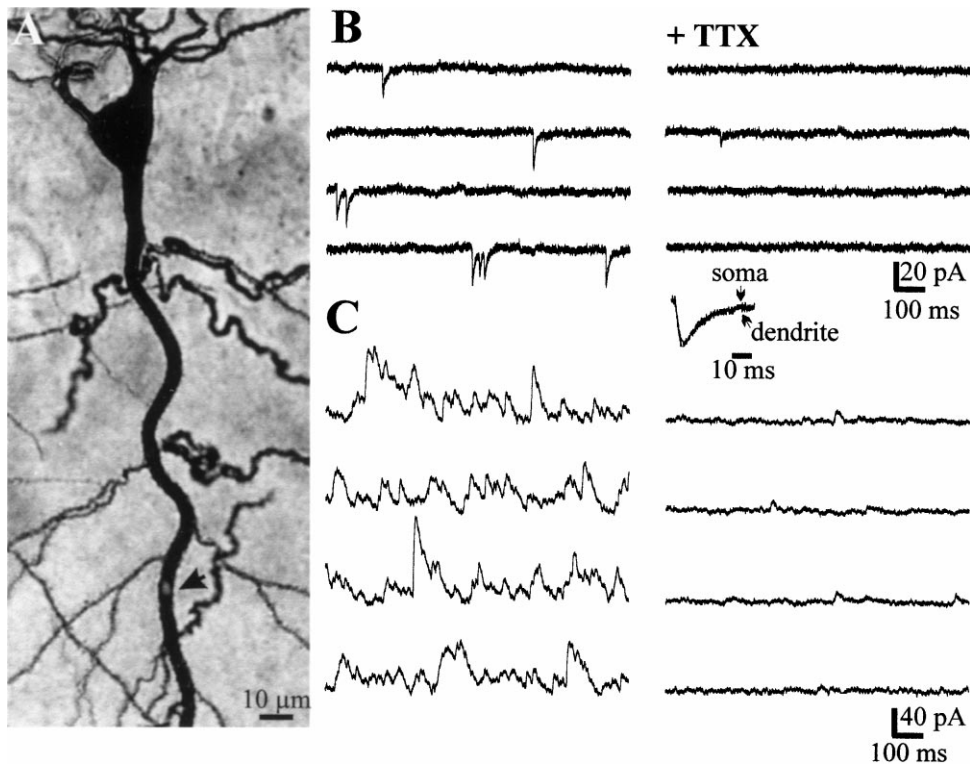


Fig. 3. Distribution of spontaneous and miniature activities in the apical dendrite of a CA1 pyramidal neuron. (A) Identification of the recording site (arrow) in the apical dendrite. (B) sEPSCs are suppressed by TTX and are thus entirely due to action potential-dependent release of transmitter. (C) The high frequency of sIPSCs recorded in control ACSF is dramatically decreased in the presence of TTX indicating that in the apical dendrites mIPSCs do not participate to spontaneous GABAergic activities. In this cell, the ratio of spontaneous IPSCs/EPSCs was 87%.

the soma. The average amplitude of mIPSCs was 15.07 ± 0.15 pA (Fig. 2F).

It could be argued that the rate of mIPSCs recorded when evoked release is blocked by TTX does not reflect the physiological rate, i.e. TTX could alleviate a physiological up- or down-regulation of miniature release. In an effort to address this issue, we have performed two additional analyses. (1) The amplitude histograms of sIPSCs and mIPSCs from five cells show that the distribution of sIPSCs of small amplitude overlaps with that of mIPSCs (Fig. 2D). This observation suggests that the rate of mIPSCs is similar with and without TTX. (2) We have measured the frequency of events when synaptic transmission was blocked by cadmium ($100 \mu\text{M}$). The distribution of GABAergic currents in cadmium was similar to that measured in cadmium plus TTX ($n = 3$, Fig. 2E).

Distribution of spontaneous and miniature currents in apical dendrites

Recording sites were $370 \pm 80 \mu\text{m}$ (range $120\text{--}480 \mu\text{m}$) away from the soma (Figs 1 and 3A). The frequency of sEPSCs in apical dendrites was significantly higher than in the somata; 2.01 ± 0.42 Hz (Fig. 3B; $n = 9$, $P < 0.01$) and was reduced by $76 \pm 3\%$ (Fig. 3B; $n = 9$, $P < 0.001$) after TTX. In contrast, the frequency of sIPSCs was not significantly different from that at the soma, 17.29 ± 2.30 Hz (Fig. 3C; $n = 9$, i.e. $89 \pm 9\%$ of the overall spontaneous synaptic activity). However, in the presence of TTX, the frequency of sIPSCs was dramatically decreased by $88 \pm 2\%$ ($P < 0.0001$; Fig. 3C; $n = 9$, Table 1). Since the distributions of mIPSC amplitudes were similar in basal and

apical dendrites, data were pooled together. The average amplitude of mIPSCs was smaller in dendrites (12.82 ± 0.20 pA) than in somata (Fig. 2F, $P < 0.001$ Kolmogorov–Smirnov test), but their kinetics (normalized averages) were similar (Fig. 2F inset).

Distribution of spontaneous and miniature currents in basal dendrites

Recording sites were $60 \pm 20 \mu\text{m}$ away from the soma (Fig. 4A). The frequencies of sEPSCs and sIPSCs in basal dendrites were not statistically different from those recorded in the soma, 0.43 ± 0.10 Hz and 21.15 ± 3.99 Hz respectively (Fig. 4B, C; $n = 6$), showing that spontaneous activity was essentially GABAergic ($96 \pm 2\%$). TTX decreased the frequency of sEPSCs and sIPSCs by $84 \pm 3\%$ and $81 \pm 3\%$, respectively (Fig. 4B, C; $n = 6$, Table 1, $P < 0.001$ and $P < 0.0001$, respectively) as in apical dendrites.

Distribution of spontaneous and miniature currents in somata of ectopic pyramidal cells

Basal dendrites proved to be very difficult to record from. Most of the seals (90%) were made on glial cells. The remaining 10% were divided equally into basal dendrites and somata of ectopic pyramidal cells (Fig. 5A). In contrast to eutopic somata, i.e. somata in stratum pyramidale, the frequencies of sEPSCs and sIPSCs were significantly higher in ectopic cells, 1.96 ± 0.56 Hz (Fig. 5B; $n = 5$, $P < 0.01$) and 32.09 ± 7.78 Hz (Fig. 5C; $n = 5$, $P < 0.01$) respectively. However, spontaneous GABAergic activity was still predominant ($93 \pm 2\%$ of the overall activity). In the presence

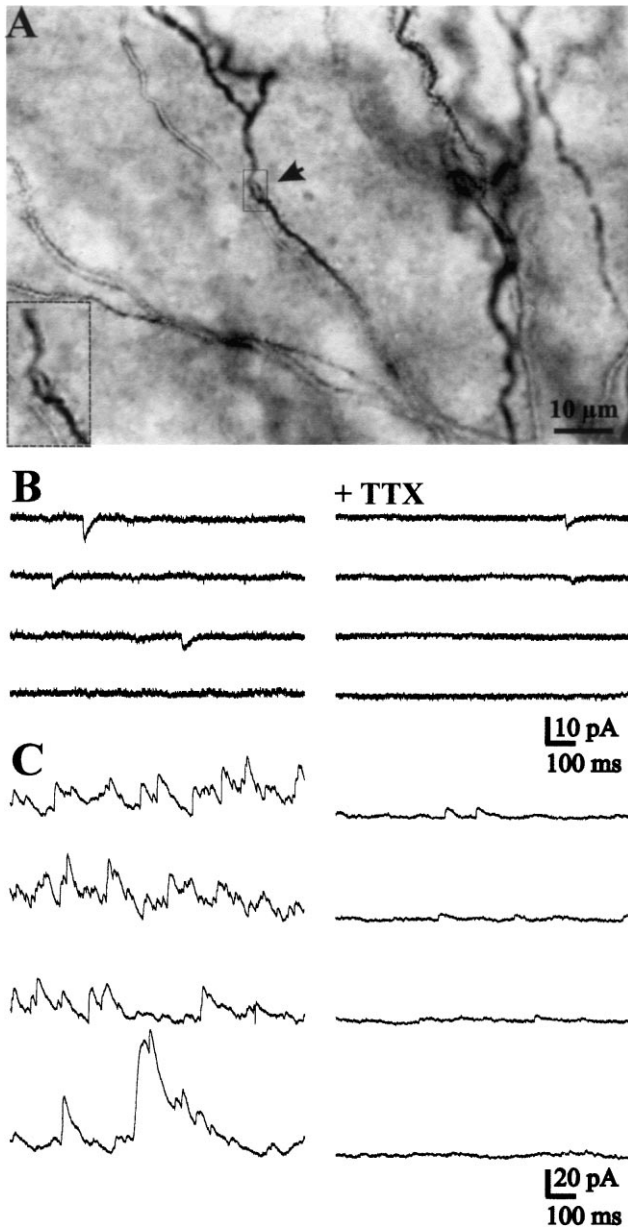


Fig. 4. Distribution of spontaneous and miniature activities in a basal dendrite of a CA1 pyramidal neuron. (A) Identification of the recording site (arrow) in a basilar dendrite. Inset: enlargement of the recording site. In basal dendrites sEPSCs (B) and sIPSCs (C) are almost exclusively due to action potential-dependent release of transmitter. In this cell, the ratio of spontaneous IPSCs/EPSCs was 92%.

of TTX, mEPSCs accounted for $10 \pm 4\%$ of the spontaneous glutamatergic activity (Fig. 5B, $P < 0.001$) and the frequency of sIPSCs was decreased to 11.41 ± 2.06 Hz (Fig. 5C; $n = 5$, $27 \pm 8\%$ of control, $P < 0.0001$). Thus, mIPSCs are also present in ectopic somata although percentage of sIPSCs is significantly smaller than in eutopic somata ($P < 0.001$).

Theoretical analysis of the signals generated and detected at different synaptic sites

The interpretation of the experimental results depends upon the site of origin of the recorded currents. In order to illustrate the possible contamination of local events (close to the recording site) by more distally generated events; we have

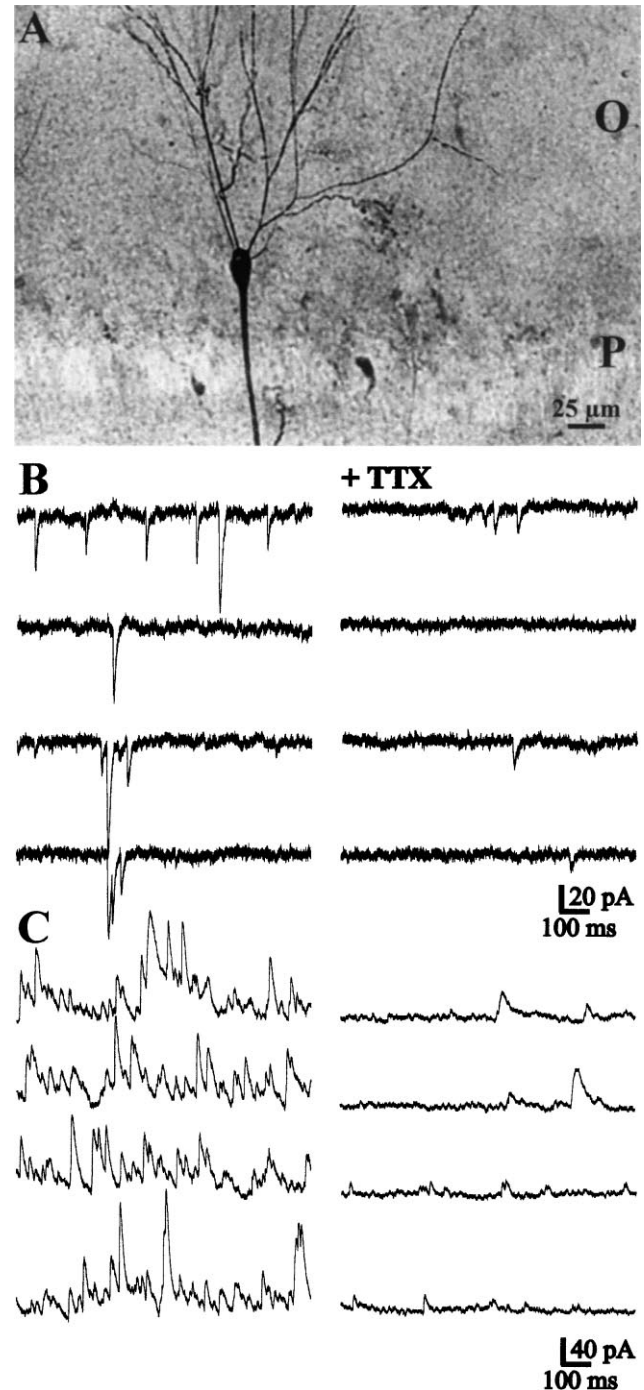


Fig. 5. Distribution of spontaneous and miniature activities in the soma of an ectopic CA1 pyramidal neuron. (A) Identification of the ectopic pyramidal soma in stratum oriens. Spontaneous EPSCs (B) and IPSCs (C) are almost exclusively due to action potential-dependent release of transmitter. Note the large spontaneous EPSCs representative of recordings from ectopic somata of pyramidal neurons. In this cell, the ratio of spontaneous IPSCs/EPSCs was 95%.

used a “realistic” simulation of an experiment including an imperfect space clamp. The set of parameters was chosen in order to achieve the highest level of detectable contamination. We have addressed three questions with the model: (i) how far away can somatic events be detected in the various dendritic branches; (ii) how far away can a dendritic recording pick up synaptic activity and; (iii) what is the extent of contamination of somatic recordings by dendritic events?

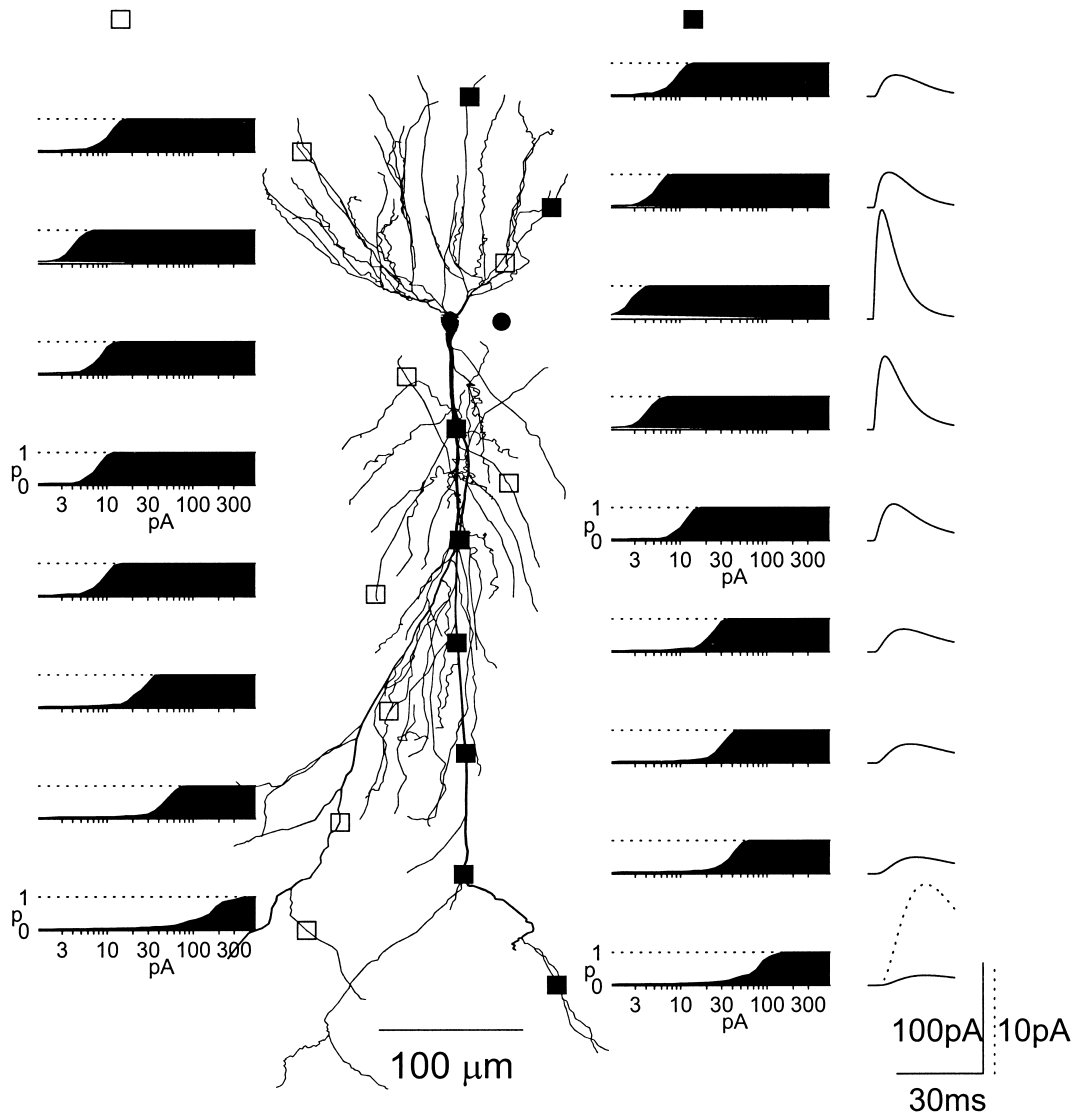


Fig. 6. Theoretical analysis of the role of electrotonic filtering in the detection of somatic currents at various dendritic recording sites in a CA1 pyramidal neuron. Projection of a biocytin filled neuron reconstructed in 3D (axon not shown). Recording sites are shown by open or filled squares. The sites where the synaptic events are generated are shown by open or filled circles. A filled symbol indicates a main dendritic branch location, an open symbol, a secondary or tertiary side branch. For each site the detection probability is shown as a function of the event amplitude in its own graph, those on the left correspond to the open circles; those on the right to the filled circle at the same level. The membrane was voltage clamped at +10 mV at the recording site (same type of display used in Figs 7 and 8). IPSCs are generated in the soma (filled circle) and recorded at various sites in the dendrites (open and filled squares). The abscissa on each subplot shows the magnitude, in pA, of the somatic IPSC. The ordinate (range 0–1) is the probability that an event of this magnitude, once filtered and subject to recording noise (see experimental procedures) is registered at the dendritic recording site. For the right-hand column, the time-course of an IPSC with an amplitude of 100 pA generated in the soma is shown at various recording sites. Small events are rescaled (dotted line). Note that, except for recording sites on or close to the first 300 μm of the apical dendrite, events smaller than 20 pA (average amplitude of mIPSC) have a very low probability of detection.

Simulations of the detection probability of IPSCs generated in the soma when recording from a dendrite, of dendritic IPSCs recorded in the dendrites and of dendritic IPSCs recorded at the soma, respectively are shown in Figs 6–8. The cell was held at +10 mV at the recording site through an 8 M Ω pipette and events of different amplitude were injected at the synaptic site. The detection probability for each event was computed by adding noise and using the same detection algorithm as for experimental data. The figures show this probability as a function of the amplitude the event would have if it had been recorded at the synaptic site.

For events generated in the soma and recorded in various dendritic branches (Fig. 6), only IPSCs with an amplitude larger than 40 pA have a probability greater than 0.1 to be

detected at the recording sites equivalent to the experimental ones along the main apical dendrite. The probability of recording a somatic event is even lower in lateral dendritic branches (of smaller diameter) at the same level. These simulations suggest that mIPSCs generated in the perisomatic region are rarely detected in the apical dendrites. Their amplitude needs to be greater than 40 pA, a population of events with a low probability of occurrence ($P < 0.1$, Fig. 2F). Therefore, the contamination of dendritic recordings by somatic events appears to be limited to large amplitude currents.

If the recording site on the apical dendrite is located 250 μm away from the soma, the simulation suggests that the clamp extends better toward the distal dendrites than toward the soma (Fig. 7). This is due to the fact that the

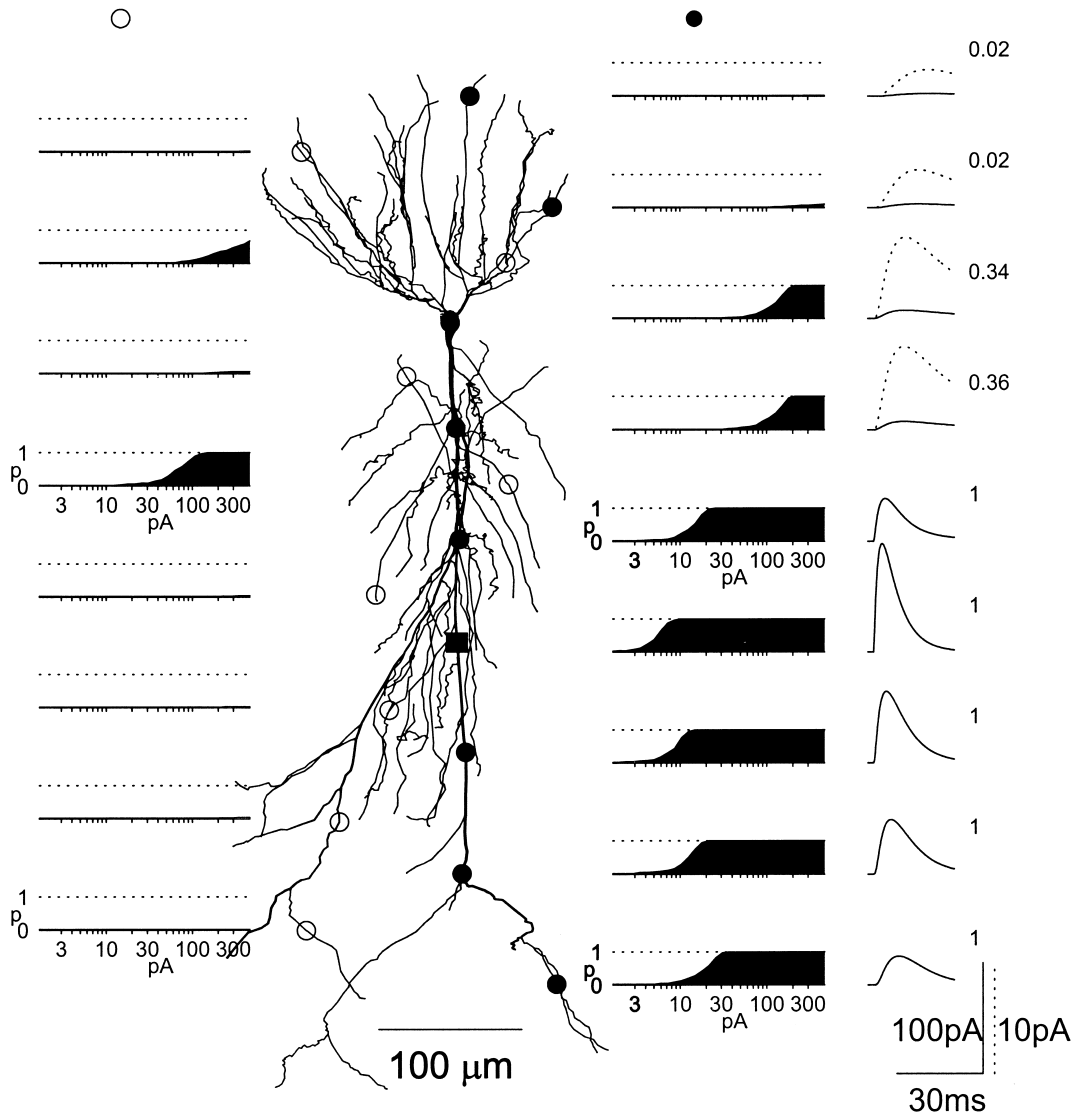


Fig. 7. Theoretical analysis of the role of electrotonic filtering in the detection of dendritic currents in the apical dendrite of a CA1 pyramidal neuron. Detection probability of IPSCs generated at various locations in the dendritic tree (open and filled circles) recorded in the apical dendrite 250 μm away from the soma (filled square). Presentation as in Fig. 6, but here the plot associated with a dendritic point shows the probability that an event at that site is registered at 250 μm away from the soma against the amplitude that would have been recorded locally. The time-courses on the right are for somatic recordings of a 100 pA dendritic event. The probability of detection is indicated. Note that the clamp extends better toward the distal part of the dendritic tree.

membrane surface area decreases toward the terminal tuft whereas it increases toward the soma. As a result the clamp falls off faster as a function of the distance toward the soma. For these reasons, synaptic events generated in most of the apical dendrite and smaller side branches directly connected would be detected 250 μm away from the soma.

Somatic recordings would pick up most IPSCs generated in the apical and basal dendrites (Fig. 8). Only distal ($>300 \mu\text{m}$) IPSCs generated in the main apical dendrites or side branches will remain undetected. However, because 90% of dendritic mIPSCs are below 20 pA (Fig. 2F), the model indicates that only dendritic mIPSCs generated within 200 μm from the soma will be recorded in the soma.

DISCUSSION

The main results of this study are that: (i) in the slice preparation, spontaneous activity is primarily GABAergic and is equally distributed in somata, apical and basal

dendrites and (ii) miniature activity is primarily GABAergic and almost entirely restricted to the perisomatic region.

Contamination of recordings by distally generated events

The synaptic currents measured at various recording sites are a mixture of locally and distally generated events. However, the contamination by distal events is limited because the entire cell cannot be adequately clamped.^{4,7,34,37,38} We have used a computer model of our experimental conditions in order to assess the theoretical level of contamination. For somatic recordings the model indicates that dendritic events of small amplitude ($<40 \text{ pA}$), which includes most dendritic miniatures, will not be detected if they are generated more than 200 μm away from the soma. Events with an amplitude greater than 40 pA can be picked up with a probability that decreases with the distance between the recording and synaptic sites and with the diameter of the dendrites. For dendritic recordings, the contamination is limited to the

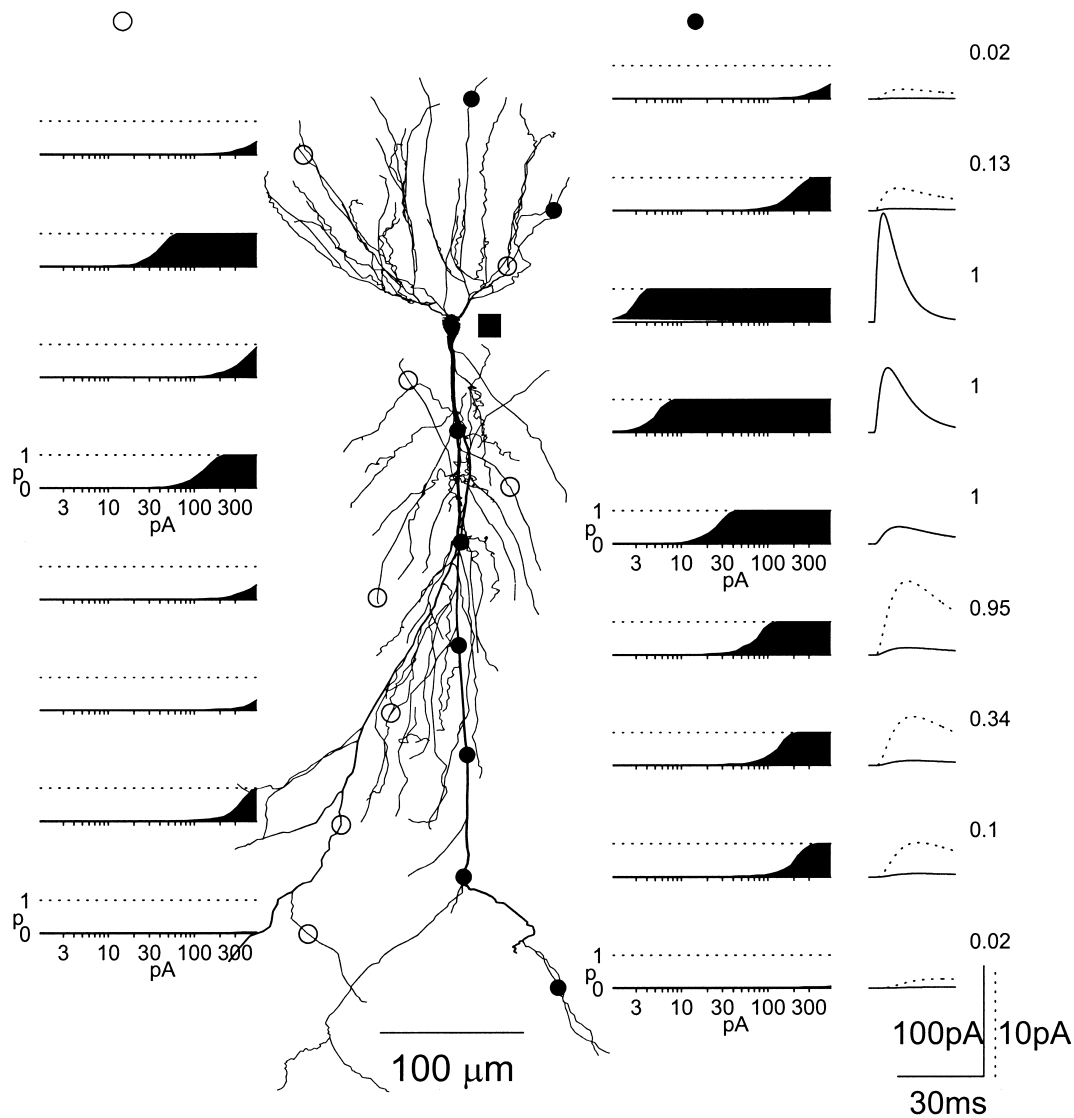


Fig. 8. Theoretical analysis of the role of electrotonic filtering in the detection of dendritic currents in the soma of a CA1 pyramidal neuron. Detection probability and time-course of dendritic events recorded at the soma. Presentation as in Fig. 7, but here the plot associated with a dendritic point shows the probability that an event at that site is registered at the soma against the amplitude that would have been recorded locally. The time-courses on the right are for somatic recordings of a 100 pA dendritic event. All these events can be detected even if they are generated in the distal dendrites.

synaptic events generated in the apical dendrite, in particular its distal part, and in the smaller side branches directly connected to it. Most mIPSCs generated in the soma cannot be recorded in the dendrites, at least at the recording locations we have used. These simulations were obtained using a conservative approach, with a set of parameters chosen in order to provide the “best” clamp of the cell. The experimental recording conditions are generally worse in terms of space clamp and filtering. Therefore, it is likely that, in these large adult neurons, the recorded excitatory and inhibitory drives correspond principally to events generated within 200 μm of the recording site.

Spontaneous activity along the somato-dendritic axis

Based on somatic recordings, previous studies reported a wide range of frequencies for sEPSCs and sIPSCs recorded in the presence of GABA and glutamate antagonists, respectively.^{5,6,11,19,23,25,30–32} Our recordings of sEPSCs and sIPSCs performed in the same neuron and in physiological

conditions indicate that the spontaneous GABAergic and glutamatergic drives account for 90% and 10%, respectively of the overall spontaneous activity. Two arguments could explain the low frequency of the excitatory drive in the slice preparation: (i) the tonic inhibition received by excitatory neurons would silence them;²⁵ and (ii) excitatory pathways are either too diffuse like the CA1 associational pathway¹³ or massively cut off from their originating somata like the Schaffer collaterals.² However, the spontaneous drive may be different *in vivo* where the connectivity is preserved.²⁶

In our experimental conditions, the glutamatergic neurons directly connected to the CA1 pyramidal neurons are the CA3 pyramidal cells (via the Schaffer collaterals) and the CA1 pyramidal cells (via the CA1 associational pathway). The latter being too diffuse,¹³ its contribution to the spontaneous glutamatergic drive recorded in CA1 pyramidal cells is likely to be marginal. It is worth noticing that the frequency of sEPSCs was higher in the soma of pyramidal cells displaced in stratum oriens (ectopic pyramidal cells) than in the soma of eutopic pyramidal cells. These excitatory inputs could

originate from the few axonal collaterals of CA1 pyramidal cells which are present in stratum oriens but not in stratum radiatum.¹⁴ The Schaffer collateral pathway is characterized by a remarkable segregation of the distribution of the synaptic contacts according to the transverse location of the emitting CA3 pyramidal cell.² Distal CA3 pyramidal cells (close to the CA1 border) mainly project to stratum oriens whereas proximal CA3 pyramidal cells (close to the hilus) mainly project to the upper part of stratum radiatum.² However, it is difficult to conclude that the greater frequency of sEPSCs measured in the apical dendrites reflects a greater firing/release probability of proximal CA3 pyramidal cells. The non-laminar projection from CA3 to CA1² adds a further level of complexity to the interpretation of these results. This issue could be addressed in the intact hippocampal preparation *in vitro* where all the connectivity is preserved.²¹ Although during steady-state conditions spontaneous GABAergic activity seems quantitatively evenly distributed in the basal dendrites, somata and apical dendrites of pyramidal cells, this inhibitory drive is qualitatively heterogeneous. It essentially depends upon the firing of basal and apical dendrite-projecting interneurons, whereas perisomatic inhibition is mostly activity-independent.

Miniature activity along the somato-dendritic axis

It is currently assumed that miniature activity following TTX is also present in the spontaneous activity measured in physiological condition.¹⁹ However, it could be argued that an up- or down-regulation of miniature activity occurs in the absence of TTX, in particular calcium-dependent mechanisms. Our observations that: (i) the distribution of small amplitude sIPSCs (probably mIPSCs) is similar to the distribution of mIPSCs measured in TTX; and (ii) the distributions of IPSCs measured in cadmium and cadmium + TTX are similar, are consistent with the hypothesis that miniature activity measured in TTX is also present in the absence of TTX.

After TTX treatment, the frequency of sEPSCs was decreased by 80% in somata and dendrites, in keeping with the value (75%) measured in the soma of adult CA1 pyramidal cells.¹⁹ These results suggest that glutamatergic presynaptic terminals have a low probability of producing miniatures *in vitro*. Future studies will have to determine whether the ability to generate mEPSCs is excitatory pathway-specific.

After TTX treatment, most (>90%) of the GABAergic activity measured in the dendrites was abolished whereas as much as 60% of the GABAergic activity remained in the soma. The origin of this difference is unclear. If the release probabilities of perisomatic and dendritic GABAergic

presynaptic terminals are similar, one possible explanation would be that perisomatic interneurons fire spontaneously less frequently than dendritic projecting interneurons. As a result, the ratio between sIPSCs and mIPSCs should be shifted toward mIPSCs in the soma. Alternatively, differences in the probability of release could be involved. Two arguments indirectly support this proposal. Miniature IPSCs recorded in the soma of dentate granule cells mainly originate from perisomatic terminals.³³ Perisomatic GABAergic terminals are structurally different since they are larger and contain more synaptic vesicles than dendritic ones.²⁴ It is possible that the probability of action potential-independent release of GABA is linked to the number of vesicles available in the presynaptic terminal.¹⁷ If this is true then the low rate of mIPSCs in stratum oriens ectopic soma of pyramidal cells as compared to eutopic cells could mean that these ectopic soma are mostly contacted by terminals arising from dendritic projecting interneurons since only very few basket and axo-axonic cell terminals are present in stratum oriens.¹⁰ A comparable “ultrastructural size principle” has been suggested for excitatory synapses.²⁸ The experimental protocol did not allow us to test these hypotheses. A dedicated study is needed to address this important issue.

In conclusion, the present observations confirm and extend the concept of two anatomically¹⁶ and functionally^{3,24} segregated inhibitory systems that regulate principal cell activity in the hippocampus. In dendrites, the spatial distribution of inhibitory contacts is fundamentally important for the processing of excitatory information (see ref. 16). In contrast, the perisomatic area can be seen as an extremely compact integrative unit where the spatial distribution of synapses is less important. The primary role of perisomatic inhibition appears to be the control of the output of the cell.^{15,24} During steady-state, the inhibitory drive is mostly tonic, which constitutes a very efficient and economical way to silence pyramidal cells. During transients, perisomatic inhibition is ideally located to generate oscillations in principal cells, (see ref. 16). In contrast, dendritic inhibition seems to be essentially dependent upon the firing of dendritic-projecting interneurons. Alterations in the properties of dendritic and perisomatic inhibition may have drastic consequences on the integrative properties of principal cells in pathologies such as temporal lobe epilepsies where dendritic projecting interneurons degenerate¹⁸ and where perisomatic mIPSC activity is massively decreased.¹⁷

Acknowledgements—Supported by INSERM, The Foundation Simone and Cino del Duca, ALLIANCE program and WELCOME TRUST. R. Cossart was a recipient of a doctoral fellowship from Ministère de l'Enseignement Supérieur et de la Recherche.

REFERENCES

1. Ali A. B., Bannister A. P. and Thomson A. M. (1999) IPSPs elicited in CA1 pyramidal cells by putative basket cells in slices of adult rat hippocampus. *Eur. J. Neurosci.* **11**, 1741–1753.
2. Amaral D. and Witter M. (1989) The three-dimensional organization of the hippocampal formation: a review of anatomical data. *Neuroscience* **31**, 571–591.
3. Andersen, P. (1990). In *Progress in Brain Research* (eds Zimmer J. and Ottersen O.). Elsevier, New York, vol. 83.
4. Andersen P., Storm J. and Wheal H. V. (1987) Thresholds of action potentials evoked by synapses on the dendrites of pyramidal cells in the rat hippocampus *in vitro*. *J. Physiol., Lond.* **383**, 509–526.
5. Banks M. I., Li T. B. and Pearce R. A. (1998) The synaptic basis of GABA_A, slow. *J. Neurosci.* **18**, 1305–1317.
6. Behrends J. C. and Ten Bruggencate G. (1993) Cholinergic modulation of synaptic inhibition in the guinea pig hippocampus *in vitro*: Excitation of GABAergic interneurons and inhibition of GABA-release. *J. Neurophysiol.* **69**, 626–629.
7. Benke T. A., Luthi A., Isaac J. T. and Collingridge G. L. (1998) Modulation of AMPA receptor unitary conductance by synaptic activity. *Nature* **393**, 793–797.

8. Bernard C., Cannon R. C., Ben-Ari Y. and Wheal H. V. (1997) Model of spatio-temporal propagation of action potentials in the Schaffer collateral pathway of the CA1 area of the rat hippocampus. *Hippocampus* **7**, 58–72.
9. Buhl E. H., Halasy K. and Somogyi P. (1994) Diverse sources of hippocampal unitary inhibitory postsynaptic potentials and the number of synaptic release sites. *Nature* **368**, 823–828.
10. Buhl E. H., Han Z. S., Lorinczi Z., Stezhka V. V., Karnup S. V. and Somogyi P. (1994) Physiological properties of anatomically identified axo-axonic cells in the rat hippocampus. *J. Neurophysiol.* **71**, 1289–1307.
11. Cohen G. A., Doze V. A. and Madison D. V. (1992) Opioid inhibition of GABA release from presynaptic terminals of rat hippocampal interneurons. *Neuron* **9**, 325–335.
12. Cossart R., Esclapez M., Hirsch J. C., Bernard C. and Ben-Ari Y. (1998) GluR5 kainate receptor activation of interneurons increases tonic GABAergic inhibition in pyramidal cells. *Nature Neurosci.* **1**, 470–478.
13. Deuchars J. and Thomson A. M. (1996) CA1 pyramidal-pyramid connections in rat hippocampus *in vitro*: dual intracellular recordings with biocytin filling. *Neuroscience* **74**, 1009–1018.
14. Esclapez M., Hirsch J. C., Ben-Ari Y. and Bernard C. (1999) Newly formed excitatory pathways provide a substrate for hyperexcitability in experimental temporal lobe epilepsy. *J. comp. Neurol.* **408**, 449–460.
15. Esclapez M., Hirsch J. C., Khazipov R., Ben-Ari Y. and Bernard C. (1997) Operative GABAergic inhibition in hippocampal CA1 pyramidal neurons in experimental epilepsy. *Proc. natn. Acad. Sci. USA* **94**, 12,151–12,156.
16. Freund T. F. and Buzsáki G. (1996) Interneurons of the hippocampus. *Hippocampus* **6**, 347–470.
17. Hirsch J. C., Agassandian C., Merchán-Pérez A., Ben-Ari Y., DeFelipe J., Esclapez M. and Bernard C. (1999) Deficit of quantal release of GABA in experimental temporal lobe epilepsy. *Nature Neurosci.* **2**, 499–500.
18. Houser C. R. and Esclapez M. (1996) Vulnerability and plasticity of the GABA system in the pilocarpine model of spontaneous recurrent seizures. *Epilepsy Res.* **26**, 207–218.
19. Hsia A. Y., Malenka R. C. and Nicoll R. A. (1998) Development of excitatory circuitry in the hippocampus. *J. Neurophysiol.* **79**, 2013–2024.
20. Johnston D., Magee J. C., Colbert C. M. and Christie B. R. (1996) Active properties of neuronal dendrites. *A. Rev. Neurosci.* **19**, 165–186.
21. Khalilov I., Esclapez M., Medina I., Aggoun D., Lamsa K., Leinekugel X., Khazipov R. and Ben-Ari Y. (1997) A novel *in vitro* preparation: the intact hippocampal formation. *Neuron* **19**, 743–749.
22. Li X. -G., Somogyi P., Ylinen A. and Buzsáki G. (1994) The hippocampal CA3 network: An *in vivo* intracellular labeling study. *J. comp. Neurol.* **339**, 181–208.
23. Manabe T., Renner P. and Nicoll R. (1992) Postsynaptic contribution to long-term potentiation revealed by the analysis of miniature synaptic currents. *Nature* **355**, 50–55.
24. Miles R., Toth K., Gulyás A. I., Hajos N. and Freund T. F. (1996) Differences between somatic and dendritic inhibition in the hippocampus. *Neuron* **16**, 815–823.
25. Otis T. S., Staley K. J. and Mody I. (1991) Perpetual inhibitory activity in mammalian brain slices generated by spontaneous GABA release. *Brain Res.* **545**, 142–150.
26. Pare D., Lebel E. and Lang E. J. (1997) Differential impact of miniature synaptic potentials on the soma and dendrites of pyramidal neurons *in vivo*. *J. Neurophysiol.* **78**, 1735–1739.
27. Parra P., Gulyás A. I. and Miles R. (1998) How many subtypes of inhibitory cells in the hippocampus? *Neuron* **20**, 983–993.
28. Pierce J. P. and Lewin G. R. (1994) An ultrastructural size principle. *Neuroscience* **58**, 441–446.
29. Prince D. A., Jacobs K. M., Salin P. A., Hoffman S. and Parada I. (1997) Chronic focal neocortical epileptogenesis: Does disinhibition play a role? *Can. J. Physiol. Pharmac.* **75**, 500–507.
30. Raastad M., Storm J. and Andersen P. (1992) Putative single quantum and single fibre excitatory postsynaptic currents show similar amplitude range and variability in rat hippocampal slices. *Eur. J. Neurosci.* **4**, 113–117.
31. Ropert N., Miles R. and Korn H. (1990) Characteristics of miniature inhibitory postsynaptic currents in CA1 pyramidal neurons of rat hippocampus. *J. Physiol., Lond.* **428**, 707–722.
32. Sayer R., Redman S. and Andersen P. (1989) Amplitude fluctuations in small EPSPs recorded from CA1 pyramidal cells in the guinea-pig hippocampal slice. *J. Neurosci.* **9**, 840–850.
33. Soltesz I., Smetters D. K. and Mody I. (1995) Tonic inhibition originates from synapses close to the soma. *Neuron* **14**, 1273–1283.
34. Spruston N., Jaffe D., Williams S. and Johnston D. (1993) Voltage- and space-clamp errors associated with the measurement of electronically remote synaptic events. *J. Neurophysiol.* **70**, 781–802.
35. Stuart G. J., Dodt H. U. and Sakmann B. (1993) Patch-clamp recordings from the soma and dendrites of neurons in brain slices using infrared video microscopy. *Pflügers Arch.* **423**, 511–518.
36. Tsubokawa H. and Ross W. N. (1996) IPSPs modulate spike backpropagation and associated [Ca²⁺]_i changes in the dendrites of hippocampal CA1 pyramidal neurons. *J. Neurophysiol.* **76**, 2896–2906.
37. Turner D. (1988) Waveform and amplitude characteristics of evoked responses to dendritic stimulation of CA1 guinea-pig pyramidal cells. *J. Physiol., Lond.* **395**, 419–439.
38. Turner D. A. (1984) Conductance transients onto dendritic spines in a segmental cable model of hippocampal neurons. *Biophys. J.* **46**, 85–96.

(Accepted 5 May 2000)